EFFECTS OF SURFACE CURVATURE AND SURFACE CHARACTERISTICS OF CARBON-BASED NANOMATERIALS ON THE ADSORPTION AND ACTIVITY OF ACETYLCHOLINESTERASE

Tina Mesarič[1#], Lokesh Baweja[2#], Barbara Drašler[1], Damjana Drobne[1,3,4], Darko Makovec[4,5], Peter Dušak[5], Alok Dhawan[2,6], Kristina Sepčić[1*]

[1]*University of Ljubljana, Biotechnical Faculty, Department of Biology, Večna pot 111, Ljubljana, Slovenia*

[2]*Nanomaterial Toxicology Group, CSIR-Indian Institute of Toxicology Research, Council of Scientific and Industrial research (CSIR), Mahatma Gandhi Marg, P.O. Box 80, Lucknow-226001, Uttar Pradesh, India*

[3]*Centre of Excellence in Advanced Materials and Technologies for the Future (CO NAMASTE), Ljubljana, Slovenia*

[4]*Centre of Excellence in Nanoscience and Nanotechnology, Ljubljana, Slovenia*

[5]*Institute Jožef Stefan, Jamova 39, Ljubljana, Slovenia*

[6]*Institute of Life sciences, School of Science and Technology, Ahmedabad University, University Road, Ahmedabad-380009, Gujarat, India*

[#] These authors contributed equally to this study.

*Corresponding author. Tel: +38613203419, Fax: +38612573390. E-mail address: kristina.sepcic@bf.uni-lj.si (K. Sepčić)

Abstract

Carbon-based nanomaterials (NM) are promising candidates for a myriad of applications ranging from drug delivery to biosensing platforms. In the physiological environment, proteins can be adsorbed onto the surface of NM that can alter their structure and function. Little is known of the effect of NM on larger proteins and enzymes and an attempt has been made in this study to investigate the effect of carbon-based NM such as carbon black (CB), graphene oxide (GO) and fullerene (C_{60}) on the adsorption and activity of acetylcholinesterase (AChE), a key enzyme present in brain, blood and nervous system and a suitable neurotoxicity biomarker. Experimental and computational results showed that all the carbon-based NM tested adsorb AChE but they have different effects on the catalytic activity of the enzyme. The most efficient AChE inhibitor is CB. In contrast, AChE adsorbed on the GO surface retains its native conformation and most of its activity. As compared to GO and CB, C_{60} was found to be an inefficient adsorbent of AChE. The distinctive adsorption pattern of NM and their inhibitory potential could be related to the surface characteristics of NM. Our studies also demonstrate the potential of GO as a substrate for immobilization of AChE.

1. Introduction

Carbon-based nanomaterials (NM), with their unique physiochemical properties [1,2], have emerged in recent years as promising candidates for drug delivery systems, cellular imaging, biosensor matrices, and other biomedical applications. In the course of these applications, NM are liable to be exposed to a complex milieu of proteins and enzymes present in the physiological environment and these proteins and enzymes can be adsorbed onto the surface of NM. This adsorption in turn depends mainly upon the size, curvature and surface chemistry of NM [3]. There have been extensive studies on the adsorption of proteins onto NM which, it has been shown, can affect both the structure and function of proteins. The adsorption of proteins on the surface of NM is often accompanied with the loss of proteins' native conformation, and this is a major concern in the development of the potential of NM in various applications. Among carbon-based NM, the carbon nanotubes (CNT) and graphene have the capability to disrupt the α-helical structures of short peptides, and due to its low surface curvature, graphene possesses the additional capability to distort α–helical conformations [4]. Moreover, the single-walled carbon nanotubes (SWCNT) can lodge in the hydrophobic cores of signalling and pathway-regulatory proteins to form stable complexes [5]. The recent studies by Zuo et al. [6] showed that the adsorption of the protein villin depends upon the surface curvature of carbon-based NM. It is unclear however how NM can affect enzymes and larger proteins with complex tertiary structure.

It has recently been shown that the NM can interact with and inhibit the activity of acetylcholinesterase (AChE) [7], which is found on the extracellular surfaces of neurons and erythrocytes [8]. AChE hydrolyses the neurotransmitter acetylcholine, thus regulating the proper functioning of the muscle system. This reaction takes place at catalytic site of the

enzyme that is deeply buried at the bottom of a narrow cavity 20 Å in length which is referred to as the active-site gorge. Over 60% of the surface of this gorge is covered by conserved aromatic residues [9]. Of the NM that have been studied, the CNT are the most potent inhibitors of this enzyme [7] and it is of interest to study the effect on the adsorption and activity of AChE of other carbon-based NM such as carbon black (CB), graphene oxide (GO) and fullerene (C_{60}) which have different surface curvatures and surface chemistry. The fullerene family, particularly C_{60}, has useful photo-, electrochemical and physical properties, which can be exploited in various medical fields. The study of its biological applications has attracted increasing attention despite the low solubility of fullerenes in physiological media. However, C_{60} can form relatively stable clusters, referred to as nano $C_{60,}$ in aqueous systems [10]. Single layer graphene oxide (GO) is formed as one-atom-thick planar graphene sheets with additional oxygen-containing functional groups. Due to its unique structural, mechanical, and electronic properties, GO has attracted much research interest in nanoscience and nanotechnology and recently, some graphene-based biodevices have also been proposed [6,11,12]. Finally, nano carbon black (CB), produced by the incomplete combustion of heavy petroleum products and other biological materials, is a form of amorphous carbon with a high surface area-to-volume ratio. Carbon black NM are frequently used as model materials in studies of their oxidative capacity which in turn may lead to toxic effects [13].

In the study presented here, the adsorption and the inhibition of AChE in vertebrates and invertebrates by these NM were assessed both experimentally and computationally. The computational studies have been applied to obtain the atomistic scale information of NM-AChE interactions. It was hypothesised that the mechanism of AChE adsorption onto the CB,

GO and C_{60} would be different due to the different shapes and surface chemistry of the materials, and this would lead to differences in inhibition by and adsorption rates of AChE.

2. Experimental

2.1. Materials

C_{60} nanopowder was obtained from Sigma (USA) with nominal purity > 99,5 %, as stated by the producer. CB nanopowder was provided by PlasmaChem GmbH (Berlin, Germany) with the average size of primary particles of 13 nm. Single layer graphene oxide (GO) dispersion in MilliQ water was purchased from Graphene Supermarket (USA). According to the producer, GO was composed of carbon (79%) and oxygen (20%). Flake size was assessed as between 0.5-5 μm, and at least 80% of GO was single-sheet.

Recombinant AChE from fruit fly (*Drosophila melanogaster*) was a gift of Professor Jean-Louis Marty (Perpignan, France), while AChE from electric eel (*Electrophorus electricus*) was from Sigma (USA). All other reagents used for enzyme assays were also obtained from Sigma, and were of the highest purification grade available.

2.2. Methods

Analyses of enzyme activity after their incubation with NM are a relevant measure of the functional change in enzymes after their interaction with NM. However, the enzyme activity assays are difficult to conduct due to the interference of NM and test medium which lead to formation of NM agglomerates and therefore the suspension of NM must be carefully characterised and comparisons to other studies should be made with caution. In the study presented here, a modification of the Ellman's assay [14] for measuring AChE activity, modified as described by Wang et al., [7] was used.

2.2.1. Preparation and characterization of NM suspensions

A stock suspension of C_{60} was prepared at concentration of 1 mg/mL in MilliQ water and ultrasound-waterbath sonicated for 72 h (250W, 50 Hz; Sonis 2GT, Iskra Pio d.o.o., Slovenia) to obtain a stable suspension. A stock suspension of CB was freshly prepared in MilliQ water at a concentration of 0.5 mg/mL, sonicated (Sonics Vibra Cell, Newtown, USA) for 1 h at 40 % amplitude and 15 sec on/15 sec off cycle, cooling the suspension in ice. The original solution of GO, obtained by the producer, was used as stock, at a concentration of 275 μg/mL. For transmission electron microscopy (TEM) investigations, the materials were deposited by drying their water suspension on a copper-grid-supported transparent carbon foil. TEM analysis was performed with a JEOL 2100 microscope operated at 200 kV. The ζ-potential of the carbon-based NM dispersed in MilliQ water or in the reaction mixture was measured using a Brookhaven Instruments Corp., ZetaPALS. The reaction mixture was composed of Ellman's reagent in 100 mM phosphate buffer, pH 8.0, and the substrate acetylthiocholine chloride at a final concentration of 500 μM. The size distributions of the particles suspended in MilliQ water or in the reaction mixture at a concentration of 10 μg/mL were determined using a dynamic light scattering (DLS) Fritsch Analisette 12 DynaSizer.

2.2.2. Estimation of acetylcholinesterase activity

Adsorption and inhibition of AChE by different NM was assayed by Ellman's method [14] adapted for microtiter plates. All the measurements were performed at 20 °C in triplicates. To assess the rate of enzyme inhibition, 50 μL of either *D. melanogaster* or *E. electricus* AChE, dissolved in 100 mM phosphate buffer, pH 8.0, in concentrations of 0.1 and 0.06 U/mL respectively, were mixed in Eppendorf tubes with 10 μL of NM suspensions (0 – 1 mg/mL) in MilliQ water in different final concentrations. After the 10 min incubation, 100 μL of

Ellman's reagent and 50 μL of the substrate acetylthiocholine chloride (2 mM) were added to each tube and the enzyme reaction was allowed to develop for 5 minutes. Then the tubes were centrifuged for 5 min at 12,000 *g* to separate NM-enzyme complexes from the free enzyme, and 210 μL of supernatant from the each tube was pipetted onto a microtiter plate. The absorbance at 405 nm was measured 20 min after the addition of the substrate and the Ellman's reagent to the reaction mixture, using the automatic microplate reader (Dynex technologies, USA). For each NM concentration, an appropriate blank was prepared, where the enzyme was replaced by 50 μL of 100 mM phosphate buffer pH 8.0. To test the possible effect of NM on the reaction product (5-thio-2-nitrobenzoic acid), Ellman's reagent was reduced with a minimal volume of 2-mercaptoethanol, and diluted to give the final value of absorbance at 405 nm identical to the one obtained in the enzyme reaction without the NM. 100 microliters of such solution were combined with 50 μL of 2 mM substrate, 50 μL of 100 mM phosphate buffer, pH 8.0, and 10 μL of the appropriate NM suspension.

To determine the adsorption rate of the enzyme into the NM, enzyme and NM were combined in Eppendorf tubes as described above and incubated for 10 min, during which they were centrifuged for 5 min at 12,000 *g* and the supernatants (60 μL) containing non-adsorbed enzyme pipetted onto the microtiter plate. 100 μL of Ellman's reagent and 50 μL of 2 mM substrate were added to each well and the absorbance was read at 405 nm exactly 20 min after the addition of the substrate and the Ellman's reagent to the reaction mixture.

2.2.3. Quenching of insect AChE intrinsic tryptophan fluorescence by nano carbon black and grapheme oxide

Intrinsic tryptophan fluorescence of *Drosophila melanogaster* AChE (6.5 μg/mL) in 100 mM phosphate buffer, pH 8.0, was measured on a compouter-controlled Jasco spectrometer. Measurements were made at 25 °C in a constantly stirred 1 cm path length quartz cuvette with a scan rate of 250 nm/min. Slit widths with a nominal band pass of 5 nm were used for both excitation and emission beams. The fluorescence emission spectra were recorded in the wavelength range of 300 to 450 nm after excitation with the wavelength at 295 nm to monitor only the tryptophan fluorescence emission. Since the enzyme was titrated with CB or GO (0 - 50 μg/mL) directly in the cuvette, the spectra were multiplied by a dilution factor. The apparent fluorescence emission spectra of the solvent and respective NM (background intensity) were subtracted from corresponding fluorescence emission spectra containing the mixture of NM and AChE.

2.2.4. Docking and simulation studies:

In order to gain insight into the adsorption of AChE on the surface of the selected carbon NM, computational studies were performed between the models of carbon NM and AChE. The descriptions of generated NM models and the enzyme are as follows: (i) Nano carbon black (CB) model: a carbon sheet having surface area of 25 nm^2 was build using visual molecular dynamics (VMD) builder to mimic the hydrophobic surface of CB. Recently, the carbon sheet-like models have been generated to study the effect of surface modifications of CB on the morphology and crystallization of poly(ethylene terephthalate)/CB masterbatch model [15]; (ii) Single layer graphene oxide (GO) model: the GO surface was built using a carbon sheet having the surface area of 25 nm^2, and the surface of GO was decorated with the

epoxy(-O-) and hydroxyl groups (-OH). The carboxyl (-COOH) groups were attached to the edges of the carbon sheet to mimic the GO NM [16]; (iii) fullerene C_{60} agglomerates: according to the characterization data of the tested C_{60} suspension, these NM are present in agglomerated form. Therefore, in order to elucidate the effect of C_{60} on AChE, a surface consisting of 36 C_{60} molecules was built.. Co-ordinates of human AChE (1B41) were taken from the Research Collaboratory for Structural Bioinformatics (RCSB) database. The vertebrate and invertebrate AChEs are structurally very similar [9].

2.2.4.1. Docking studies:

Docking studies have been performed using the patchdock online server to obtain the most probable adsorption site of AChE on the surface of carbon NM surfaces. The most favourable binding pose was selected on the basis of its score [17].

2.2.4.2. Simulation studies:

MD simulation studies have been widely applied in an attempt to understand the adsorption of proteins and other biomolecules on the surface of NM [18,19]. In this study, we performed MD simulations to study the adsorption of AChE on the surface of CO, GB and C_{60}, and to obtain detailed insights into the effect of these carbon NM on the conformation of AChE during adsorption. Molecular dynamics simulations were performed between AChE and NM for 5 ns in all the systems with GROMACS version 4.5.3 [20]. The force field parameters of the Optimized Potentials for Liquid Simulations (OPLS), a force field widely used for protein simulations [21], were selected to study all three systems. All the systems were solvated with single point charge (SPC) water and the simulations were carried out in an isothermal-isobaric ensemble. Nanomaterials and AChE were unconstrained throughout the simulations. The pressure was controlled at 1 atm and the temperature was retained at 300 K using Parrinelo-

Rahman Barostat and V-rescale thermostat, respectively [22]. A 2 fs time step was used to integrate the equation of motion. Electrostatic interactions were calculated using Particle Mesh Ewald sums with a non-bonded cut off at 10 Å [23]. Bonds between hydrogen and heavy atoms were constrained at their equilibrium length using the LINCS algorithm [24]. Various steps were involved including the minimization of the system with the equilibration of the whole system for 100 picoseconds (ps). A production run of 5 ns was performed in all the three systems. The trajectories were saved at 1 ps intervals for further analysis. The analysis of the trajectories were made using GROMACS suite of programs and the results were visualized using a VMD package [25].

AChE was simulated in solvent alone for 5 ns as a control. The root mean square fluctuations (RMSF) values of Cα atoms of amino acid residues were calculated calculated using g_rmsf command in GROMACS. RMSF is a measure of the deviation of the Cα of each residue with respect to a reference structure which was the average structure calculated over the MD trajectory. The RMSF analysis has been performed in previous MD simulation studies to study the conformational rearrangements and dynamics of AChE gorge residues in the presence and absence of ligands [26,27].

3. Results

3.1. *Characterization of nanomaterials*

Inspection of NM by TEM showed that CB is composed of amorphous, globular primary nanoparticles with diameters of about 20 nm. C_{60} is composed of primary nanoparticles which are frequently crystalline and have a broader size distribution than CB, ranging from approximately 20 nm to several hundred nm. Electron diffraction showed reflections corresponding to the face-centered cubic structure of C_{60}. The GO nanostructures could not be observed by conventional TEM.

Electromobility measurements showed relatively high negative ζ-potentials for all the NM suspended both in water and in reaction mixtures. In water, the ζ-potentials measured at suspensions' inherent pH of 7.1, ranged between -32 mV and -36 mV. The reaction mixture contained some solid particles, formed by precipitation, which might impede the measurements of the NM. The ζ-potential of those particles was determined to be -17 mV, significantly lower than those of the suspended NM. The CB and the GO showed comparable ζ -potentials in the reaction mixtures at pH of 7.7 and in water (-33 mV), whereas the ζ-potential of the C_{60} was somewhat lower in the reaction mixture (-20 mV) than in water.

DLS measurements of a hydrodynamic diameter of the particles present in the suspensions (10 μg/mL) showed substantial agglomeration (SI Figs. 1-2). CB suspended in water contained particles with sizes ranging between 60 nm and 170 nm, and the largest number of the particles in the distribution was about 60 nm. In the reaction mixture, the agglomeration of the CB was even more extensive; here the largest number of particles was about 110 nm in size and the size of the largest agglomerates extends into the μm range. The largest number of particles in the water suspension of C_{60} is approximately 80 nm in diameter, and some agglomerates ranging from 100 to 600 nm in diameter are also present. In the reaction mixture, C_{60} shows especially extensive agglomeration, with the agglomerates ranging from

approximately 250 nm to several μm in size. DLS analysis of the GO suspensions was not possible because of extremely anisotropic, 2D-shape of the primary particles – molecular sheets. According to the producer, at least 80% of GO was single sheet, while the sheet size varies between 0.5 and 5 μm. Because the GO molecules are highly charged, their agglomeration in the aqueous suspensions is not expected.

3.2. Adsorption and inhibition of AChE on carbon-based NM

Adsorption and inhibition rates of AChE from *Drosophila melanogaster* by different NM after a 10-min incubation is presented in Figs. 1-3. All NM tested caused adsorption and inhibition of AChE, phenomena that were both concentration-dependent. In all the cases, the rates of adsorption were larger than the inhibition rates, indicating that the inhibition of AChE activity could derive, at least partially, from the adsorption of AChE onto the surface of the NM. CB exhibited a high affinity for AChE, reaching 50% adsorption and inhibition at concentrations of 0.12 and 0.4 μg/mL respectively (Fig. 1). Total adsorption of the enzyme could be observed above 1 μg/mL of CB. The adsorption rates were quite close to the inhibition rates in all the concentrations tested, suggesting that the adsorption of the enzyme to CB surface is responsible for the loss of its activity.

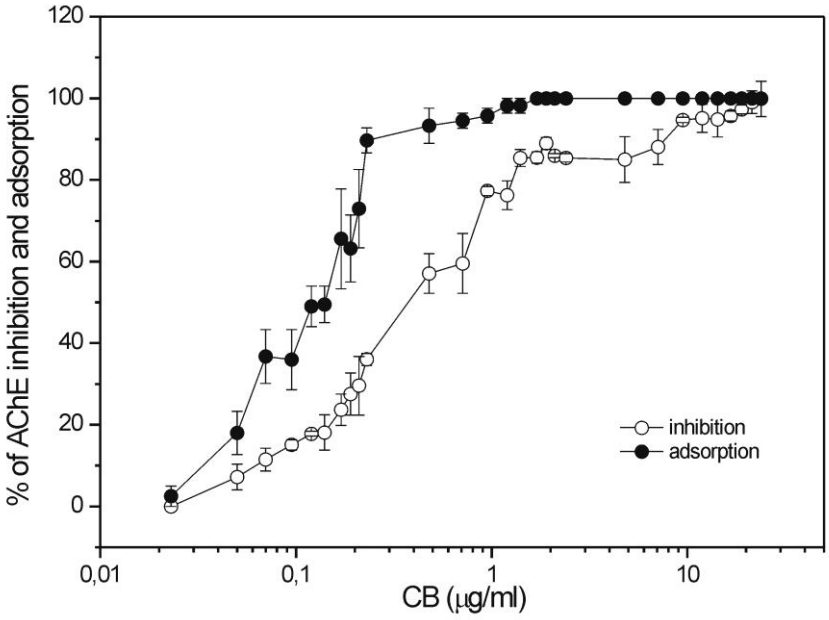

Fig. 1. Adsorption and inhibition rates of *Drosophila melanogaster* AChE by different concentrations of CB (0 – 25 μg/mL). Enzyme inhibition and its adsorption to NM after a 10-minute incubation were measured by a modified Ellman's assay, as described in the Materials and Methods section. Each point represents mean±SE of three independent experiments.

A large degree of AChE adsorption (>90%) was observed after its incubation with GO at even lower concentrations (≥0.3 μg/mL) of these NM tested (Fig. 2). In contrast to CB, the difference between adsorption and inhibition rates was much larger. For example, at an NM concentration of 10 μg/mL, at which AChE is totally adsorbed to both CB and GO, CB causes almost total inhibition of enzyme activity, while only 34% inhibition is caused by GO. These data indicate that, in contrast to CB, a fraction of the GO-adsorbed AChE still retains its enzymatic activity.

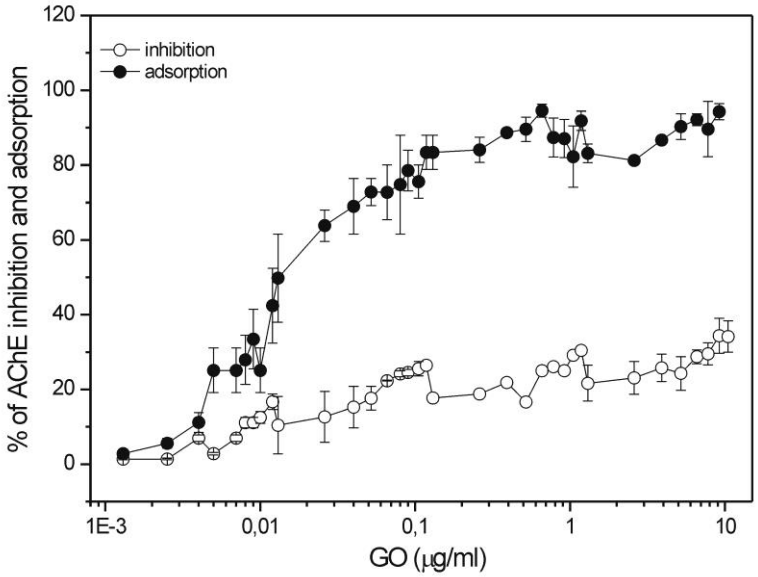

Fig. 2. Adsorption and inhibition rates of *Drosophila melanogaster* AChE by different concentrations of GO (0 – 10 μg/mL). Enzyme inhibition and its adsorption to NM after a 10-minute incubation were measured by a modified Ellman's assay, as described in the Materials and Methods section. Each point represents mean±SE of three independent experiments.

C_{60} (Fig. 3) did not show significant alterations in AChE activity, as only slight increases in adsorption and inhibition were observed at the relatively high concentrations of C_{60} tested (> 20 μg/mL).

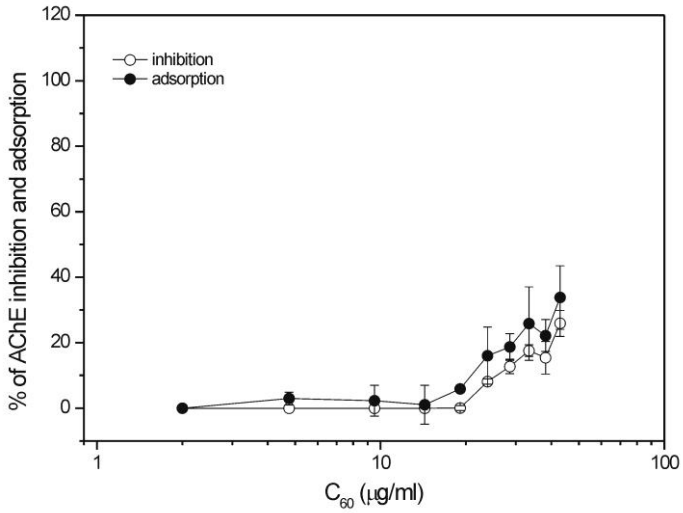

Fig. 3. Adsorption and inhibition rates of *Drosophila melanogaster* AChE by different concentrations of C_{60} (0 – 43 μg/mL). Enzyme inhibition and its adsorption to NM after a 10-minute incubation were measured by a modified Ellman's assay, as described in the Materials and Methods section. Each point represents mean±SE of three independent experiments.

The differences in sorptive and inhibitory potentials of all the three NM can also be clearly seen when comparing their LOEC (lowest observed effect concentration) values, as well as the concentrations necessary to induce 20% adsorption or inhibition of *Drosophila* AChE (EC_{20}, Table 1). Comparison of these two values clearly shows that GO adsorbs AChE at concentrations of GO that are 20-fold (LOEC), and 13.3-fold (EC_{20}) lower than those of CB, and a factor of several thousand lower than those of C_{60}. From the LOEC values, it can be

also seen that GO induces the inhibition of AChE at lowest concentrations. GO however does not induce substantial inhibition of the enzyme by increasing its concentration up to 10 μg/mL, and the inhibition pattern is completely different from that exerted by CB.

Table 1. LOEC (Lowest Observed Effect Concentration) values, and concentrations (in μg/mL) of tested carbon-based nanomaterials causing 20% inhibition and adsorption of *Drosophila melanogaster* AChE. CB, nano carbon black; GO, single layer graphene oxide; C_{60}, fullerenes C_{60}.

Nanomaterial species	**LOEC (μg/mL)**		**EC_{20} (μg/mL)**	
	inhibition	**adsorption**	**inhibition**	**adsorption**
CB	0.05	0.05	0.15±0.04	0.06±0.01
GO	0.004	0.0025	0.057±0.008	0.0045±0.001
C_{60}	25	20	40±5	30±5

Comparison of inhibition curves for these two NM (Figs. 1 and 2) shows that CB is significantly more effective in inducing rapid, concentration-dependent inhibition of AChE.

It was previously shown that different metal-, oxide-, and carbon-based NM could interact with the reactants, intermediates and products of enzymatic reactions [7,28], and these interactions should be taken into account when calculating adsorption and inhibition rates of enzymes. This however was not the case in our study since the carbon-based NM tested did not alter the absorption of the components of the reaction mixture, which was composed mainly of Ellman's reagent and its reduction product, 5-thio-2-nitrobenzoic acid.

The adsorption and inhibition rates using vertebrate AChE from the electric eel, were very similar to those obtained with the enzyme from *Drosophila melanogaster*. As shown for CB and GO in Fig. 4, slight differences in the interaction of NM with these two enzymes could be observed only at lower concentrations of NM (0.1 and 1 μg/mL), where vertebrate enzyme has been shown to be more sensitive to inhibition by CB, and more resistant to inhibition by GO.

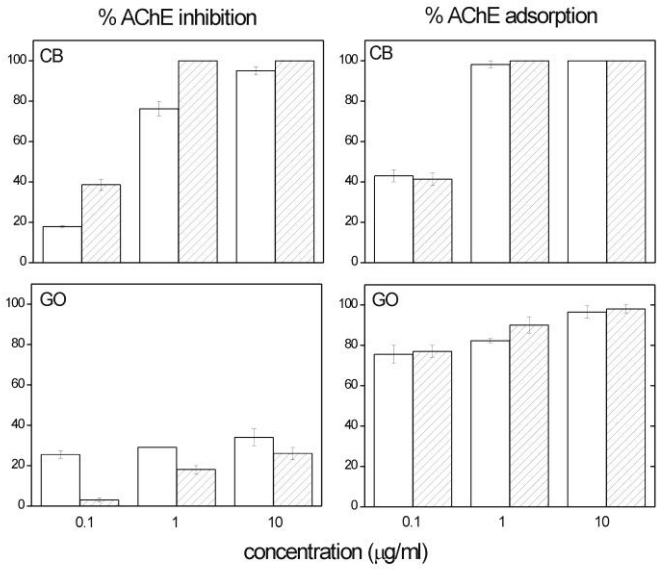

Fig. 4. Inhibition (left panels) and adsorption (right panels) rates of *Drosophila melanogaster* (open bars) and *Electrophorus electricus* (dashed bars) AChE by three different concentrations of CB and GO. Enzyme inhibition and its adsorption to NM after a 10-minute incubation were measured by a modified Ellman's assay, as described in the Materials and Methods section. Each point represents mean±SE of three independent experiments.

3.3. Quenching of intrinsic insect AChE tryptophan fluorescence by nano carbon black and graphene oxide

To assess the possible effect of CB and GO on AChE tertiary structure, *Drosophila* AChE (6.5 μg/mL) was titrated with increasing concentrations (0-50 μg/mL) of CB or GO solution, to achieve a NM:AChE ratio comparable to those used in the enzyme assays. After each addition of the NM suspension, the intrinsic tryptophan fluorescence was monitored by exciting the samples at 295 nm. The investigated enzyme contains 15 tryptophan, 26 tyrosine, and 27 phenylalanine residues, counting for 10.5% of the total amino acid content. The maximum of the emission fluorescence spectrum of AChE in 100 mM phosphate buffer, pH 8.0, was at a wavelength of 334 ± 1 nm. As shown in Figs. 5a and 5c, CB and GO induce a progressive decrease in the intensity of the emission maximum. Analysis of these data by means of a Stern-Volmer plot indicates that, upon interaction with CB or GO and adsorption to its surfaces, tryptophan residues became strongly quenched by these NM in a concentration-dependent manner (Figs. 5b and 5d).

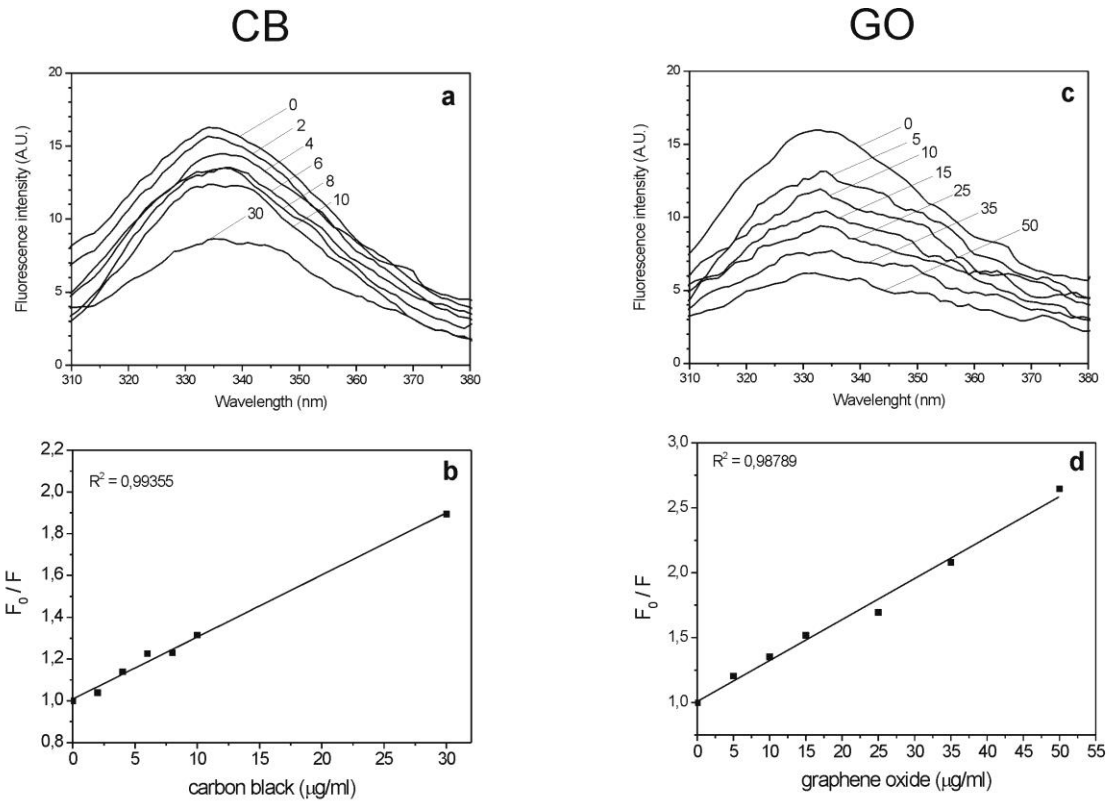

Fig. 5. Fluorescence emission spectra of insect AChE, 6.5 μg/mL, in 100 mM phosphate buffer, pH 8.0, titrated with increasing concentration of CB (**a**) or GO (**c**) (numbers indicate final concentrations in μg/mL). Excitation wavelength, λ_{exc} = 295 nm. A.U., arbitrary units. Stern-Volmer plots for quenching of intrinsic tryptophan fluorescence of soluble dimeric insect AChE by CB (**b**) and GO (**d**).

3.4. Docking and simulation studies

Docking and simulation studies revealed that carbon-based NM interact with AChE but the interactions were not in the active site region (Fig. 6a-c). Molecular dynamics (MD) simulation studies further revealed that the surface curvature and the physiochemical

properties of the nanoparticle influence the adsorption and conformational changes in AChE (SI Figs. 3-5).

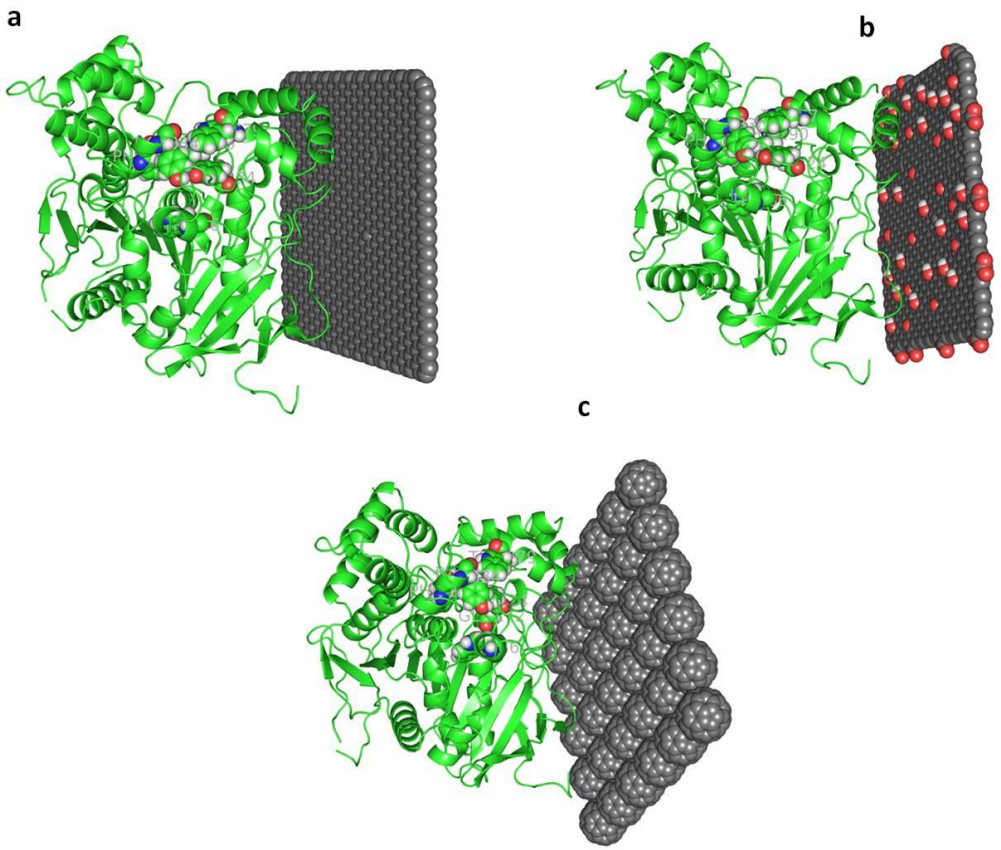

Fig. 6. Most probable interactions sites of AChE with nanomaterials obtained from docking studies. **a**) CB + AChE; **b**) GO + AChE; **c**) C_{60} + AChE. The AChE active site residues are highlighted in spherical representation.

Higher numbers of atomic contacts were formed between CB and AChE as compared to GO and C_{60} (Fig. 7).

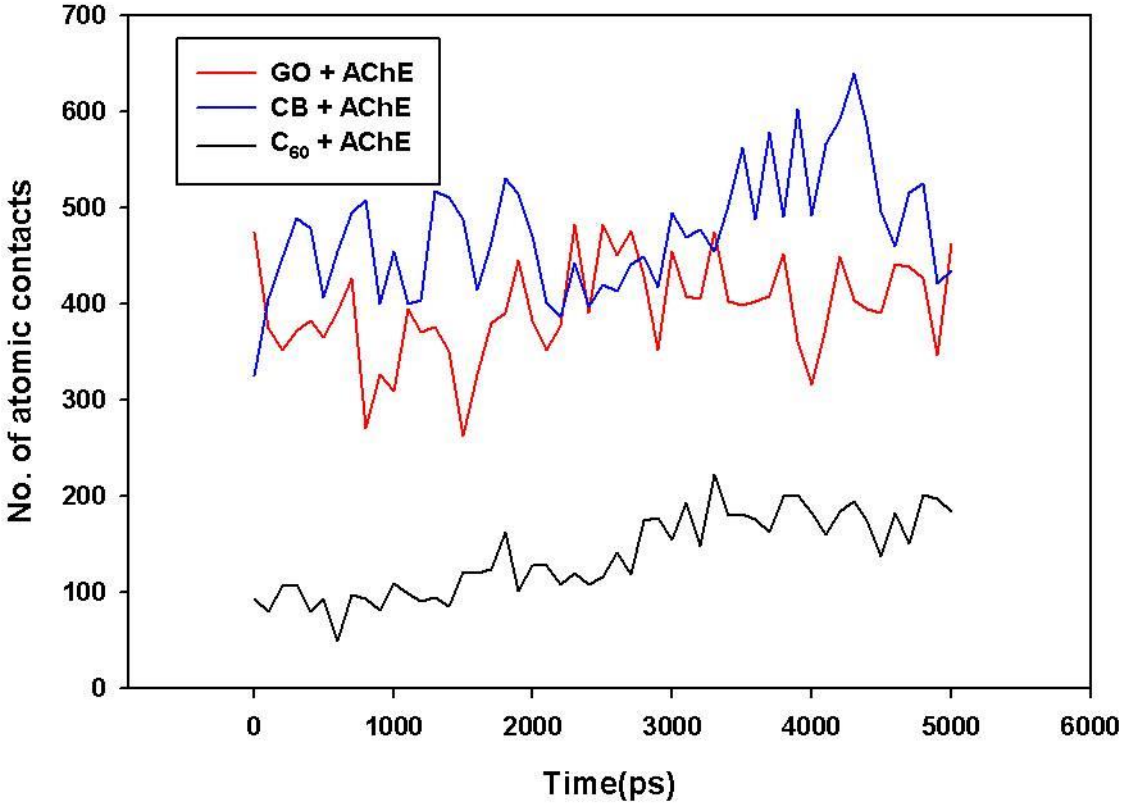

Fig. 7. Number of atomic contacts formed between AChE and tested nanomaterials during molecular dynamics simulations.

The functional groups present on the GO surface formed hydrogen bonds with amino acid residues present on the surface of AChE (Fig. 8).

After application of root mean square fluctuation (RMSF) analysis, the Cα atoms of amino acid residues present in AChE showed higher RMSF values during adsorption on CB as compared to GO and C_{60} (Fig. 9).

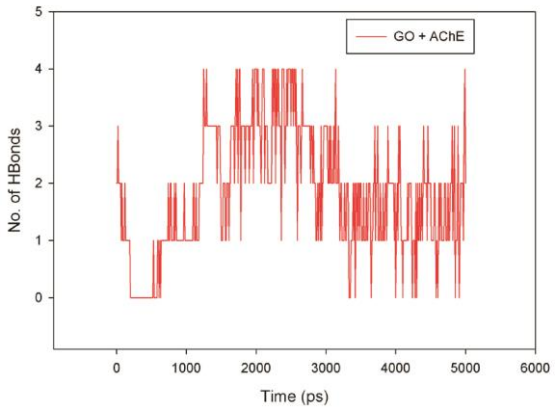

Fig. 8. Number of hydrogen bonds between AChE and GO with respect to time.

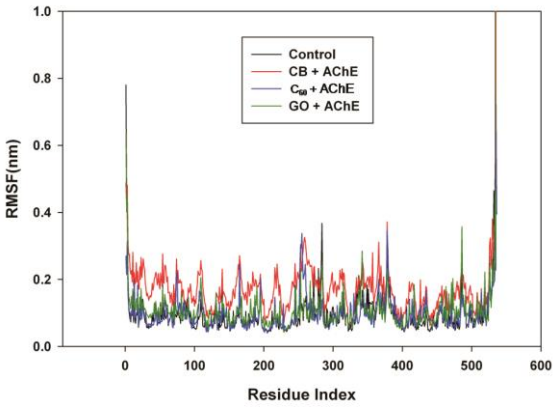

Fig. 9. Root mean square fluctuations of amino acid residues during adsorbtion of AChE on NM with respect to control simulation of AChE for 5 ns. Comparative plot of RMSF for all the system simulated is shown.

4. Discussion

4.1. Adsorption of AChE on CB, GO and C_{60}

The adsorption of proteins or enzymes over the surface of NM is a complex process and depends upon the nature of protein and physiochemical properties of the surface of NM. In this study, we have provided comparative experimental and computational data on the adsorption and potential for inhibition by carbon-based NM with either crystal or amorphous structure, different shape and secondary characteristics - size of agglomerates. We showed experimentally that the selected NM adsorb and inhibit AChE differently. In the case of CB, adsorption and inhibition were very similar while in the case of GO the majority of adsorbed enzyme remained active. Compared to CB and GO, C_{60} was found to be an inefficient adsorbent (Figs. 1-3) and the docking studies showed that the putative interaction site of AChE with NM is far away from its active site region. However, the interaction site of C_{60} with AChE is quite distinct from that of CB or GO due to the curvature of this NM. As recently demonstrated by Zuo et al., [6] the adsorption of proteins or enzymes on the surface of NM is often accompanied with the loss of the protein's native conformation. Our MD simulation studies further revealed the differential adsorption pattern and conformational changes of AChE on the carbon-based NM tested. The number of atomic contacts between AChE and CB are higher compared to GO and C_{60}. The C_{60} forms fewer contacts with AChE (SI Fig. 5) that may be attributed to the surface curvature of C_{60} molecules. These results are in close aggrement with the study of Zuo et al. [6] who showed that the adsorption of a HP 35 protein on carbon-based NM is prominent on a graphene sheet with low surface curvature, and minimal on C_{60} with its high surface curvature. In addition, it has been recently reported

that the surface topography of carbon allotropes plays a major role in adsorption of protein which also supports our study [29].

We succeeded to confirm with computational and expereimtnal approach that the adsorption on different NM surfaces induces differential conformational rearrangements in AChE. The RMSF of Cα amino acid residues of AChE in presence of NM has been compared with the RMSF values of AChE in absence of NM. This analysis clearly showed that the adsorption of AChE on CB resulted in high RMSF values, showing that the CB induced higher conformational rearrangements in AChE. However, the RMSF values in case of GO and C_{60} overlap with the values of control simulations, suggesting that the adsorption of AChE on GO failed to induce conformational changes. The differential effects of NM on the conformation of AChE arise from their different surface properties and surface curvature. With the presence of epoxides and hydroxyl groups on the surfaces, the GO is amphiphilic in nature and its edges are rich in carboxyl groups [30]. The presence of functional groups on the surface of GO leads to the hydrogen bonding and electrostatic interactions between AChE and GO, while the adsorption of AChE on CB and C_{60} is solely driven by hydrophobic and van der Waals interactions. The structural changes due to CB hydrophobic nature is evidence that hydrophobic interactions are associated with protein structural deformation [31] and is also supported by the fluoresence quenching experiment, which showed that CB can efficiently quench tryptophan residues on the AChE surface in a concentration-dependent manner.However, GO also quenched the tryptophan fluorescence (Fig. 5c). Therefore, the tryptophan quenching cannot be taken as criterion for structural changes due to location of tryptophan residues in outer and interior of the enzyme. The tryptophan residues present on

the outer surface of enzyme can easily come in contact with NM and these interactions may quench the fluoresence of tryptophan residues which may lead to erroneous conclusions.

To clarify this phenomenon we further extended the time scale of MD simulation studies up to 20 ns. The conformation obtained at the end of the simulation showed a slight loss in α-helical region of the enzyme located near CB surface. This phenomenon was not observed in case of AChE adsorption on GO (SI Figure 6). This α-helical region is closely associated with the active region of the enzyme. Therefore, any structural changes in this site of the enzyme may prevent it from proper functioning. This can be one of the mechanisms by which CB can inhibit the activity of the enzyme. Recenlty, it has been shown that CB inhbits the activity of the vital enzyme N-acetyltransferase by introducing conformational changes as well [32]. Moreover, the adsorption and inhibition of AChE by different metal-, oxide-, and carbon-based NM was assayed by Wang and co-workers on electric eel AChE [7], and on a structurally and functionally related enzyme, butyrylcholinesterase from human serum [28]. Of all the NM tested, carbon-based hydrophobic multi- and single-walled CNT were found to have the highest binding affinity for both tested enzymes, whose activity they inhibited. Similarly, in the present case, due to its highly hydrophobic nature, CB is a potent adsorber and inhibitor of the enzyme.

4.2. Effect of secondary characteristics of NM on the adsorption and inhibition of AChE

Assessing the rate of enzyme activity is a straightforward way in which to study the interaction between enzymes and NM, but the effect of the medium on NM' characteristics represents a major challenge when the effects of the agglomeration of NM on enzymes are tested. However, this is a realistic exposure scenario and to assess particle alterations in the

suspensions, and link this to their effects, it is important that particles are carefully characterised.

In this study, TEM images revealed that the primary size of both CB and C_{60} were below 100 nm in diameter with C_{60} having the broader size distribution, ranging from approximately 20 nm to several hundred nm. DLS measurements in water indicated smaller sizes of agglomerates in the case of CB suspension (ranging between 60 nm and 170 nm). For C_{60} in water, our measurements showed that the majority of the particles agglomerates were about 80 nm in diameter, with the presence of some agglomerates from 100 nm up to 600 nm. However in the reaction medium, analyses showed stronger agglomeration for both NM, extending from severeal hundreds of nm to the μm range. In the case of CB and C_{60}, no signifcant differences were observed in the sizes of agglomerates, but differences in their inhibition potential were significant. There were no significant differences in ζ-potential of three different NM, indicating that the secondary characterisitics of NM are not a significant parameter in their adsorption potential. Recently, attention has been given to studies of the interactions of agglomerates of NM on biological systems in comparison to monodispersed particles of the same size and composition [33]. This study, based on *in vitro* cytotoxicity and assessment of the uptake of monodispersed and agglomerated gold nanoparticles, reports biological activity dependent upon the presence and size of agglomerates. Consequently, differences in effects of carbon-based NM could not be ascribed solely to their chemical composition, size of particles, size of agglomerates, and stability in a suspension, but perhaps also to the shape of NM and their crystal structure [6]. This parallels our findings, that adsorption potential is shape-dependent, an observation also confirmed by other authors. The effect of NM curvature on protein adsorption was reported in the MD studies by Balamurugan

et al. [4] and Asuri et al. [34]. Mu et al. [35] provided experimental evidence that the smoother curvature of NM can induce larger protein conformational changes. This is consistent with many previous findings on spherical silica NM [36,37].

Our experimental and computational results support these studies, indicating the lowest adsorption potential for C_{60} and the significantly higher potentials of CB and GO.

4.3. Comparison of adsorption of vertebrate and invertebrate AChE on CB, GO and C_{60}

No differences were observed between vertebrate and invertebrate AChE regarding the inhibition by and adsorption to three different carbon-based NM (Fig. 4). Cholinesterases from invertebrate species are commonly classified as pseudocholinesterases, because they usually differ from vertebrate AChE in substrate specificity and different sensitivity towards specific inhibitors [38-41]. The AChE from *D. melanogaster* has a structure similar to that of vertebrate AChEs in its overall fold and charge distribution, with minor differences in the position of some surface loops and the C-terminal helix, but its active-site gorge is significantly narrower. Eight residues clustered near the opening of the gorge differ in insect and vertebrate enzymes, and are used as potential targets for inhibitor selectivity [9,42]. Similar rates of adsorption and inhibition of insect and fish AChE, obtained in our study, reinforce the hypothesis of a non-specific interaction of these enzymes with CB and GO, and support our hypothesis that the inhibition derives from the adsorption of AChE to the surface of NM and conformational changes of the enzyme.

5. Conclusion:

The study of AChE interactions with three selected carbon-based NM, performed both by monitoring the enzyme activity experimentally and by computational modelling, showed that

the adsorption of AChE is primarily influenced by the curvature of NM. Due to its highly hydrophobic nature, CB was the most potent inhibitor of AChE. The amphiphilic GO was found to be more biocompatible but unlike other NM, C_{60} was not able to interact with the AChE efficiently and this may be attributed to its high surface curvature. The present study provides information to support the safer design and development of NM for biological applications. In addition, the atomistic scale observations from this study could be useful to understand NM-mediated inhibition of enzymes. Moreover, the retention of the activity of AChE adsorbed on GO suggested the usefulness of GO as a substrate for immobilisation of this, and perhaps also other enzymes and proteins.

Acknowledgements

The authors gratefully acknowledge the Slovenian Research Agency (research project J1-4109). Funding from the European Union Seventh Framework Programme (FP7/2007-2013) under grant agreement n° 263147 (NanoValid - Development of reference methods for hazard identification, risk assessment and LCA of engineered nanomaterials) is also acknowledged. The authors also acknowledge the use of equipment in the Centre of Excellence on Nanoscience and Nanotechnology – Nanocenter. We thank Prof. Bill Milne for reading and commenting on the manuscript.

References:

[1] Zhu Z, Garcia-Gancedo L, Flewitt AJ, Xie H, Moussy F, Milne WI. A critical review of glucose biosensors based on carbon nanomaterials: carbon nanotubes and graphene. Sensors 2012; 12(5):5996-6022.

[2] Levi-Polyachenko NH, Carroll DL, Stewart JH. Applications of Carbon-Based Nanomaterials for Drug Delivery in Oncology. In: Cataldo F, Da Ros T (Editors). Carbon Materials: Chemistry and Physics, vol 1, Springer Sciences+Business Media B.V.; 2008 p. 223-226.

[3] Albanese A, Tang PS, Chang WC. The effect of nanoparticle size, shape, and surface chemistry on biological systems. Annu Rev Biomed Eng 2012; 14:1-16.

[4] Balamurugan K, Azhagiya Singam ER, Subramanian V. Effect of Curvature on the α-Helix Breaking Tendency of Carbon Based Nanomaterials. J Phys Chem 2011; 115(18):8886-92.

[5] Zuo G, Huang Q, Wei G, Zhou R, Fang H. Plugging into proteins: poisoning protein function by a hydrophobic nanoparticle. ACS Nano 2010; 4(12):7508-14.

[6] Zuo G, Zhou X, Huang Q, Fang H, Zhou R. Adsorption of villin headpiece onto graphene, carbon nanotube and C_{60}: effect of contacting surface curvatures on binding affinity. J Phys Chem 2011; 115(47):23323-28.

[7] Wang Z, Zhao J, Li F, Gao D, Xing B. Adsorption and inhibition of acetylcholinesterase by different nanoparticles. Chemosphere 2009; 77(1):67-73.

[8] Pohanka M. Cholinesterases, a target of pharmacology and toxinology. Biomed Pap Med Fac Univ Palacky Olomouc Czech Repub 2011; 155(3):219-30.

[9] Harel M, Kryger G, Rosenberry TL, Mallender WD, Lewis T, Fletcher RJ, et al. Three-dimensional structures of *Drosophila melanogaster* acetylcholinesterase and of its complexes with two potent inhibitors. Protein Sci 2000; 9(6):1063-72.

[10] Brant J, Lecoanet H, Hotze M, Wiesner M. Comparison of electrokinetic properties of colloidal fullerenes (n-C_{60}) formed using two procedures. Environ Sci Technol 2005; 39(17):6343-51.

[11] Wang K, Li HN, Wu J, Ju C, Yan JJ, Liu Q, et al. TiO_2-decorated graphene nanohybrids for fabricating an amperometric acetylcholinesterase biosensor. Analyst 2011; 136(16):3349-54.

[12] Mohanty N, Berry V. Graphene-based single-bacterium resolution biodevice and DNA transistor: interfacing graphene derivatives with nanoscale and microscale biocomponents. Nano Lett 2008; 8(12):4469-76.

[13] Koike E, Kobayashi T. Chemical and biological oxidative effects of carbon black nanoparticles. Chemosphere 2006; 65(6):946-51.

[14] Ellman GL, Courtney D, Andres V, Featherstone RM. A new and rapid colorimetric determination of acetylcholinesterase activity. Biochem Pharmacol 1961; 7:88-95.

[15] Jiang Z, Jin J, Xiao C, Li X. Effect of surface modification of carbon black (CB) on the morphology and crystallization of poly(ethylene terephthalate)/CB masterbatch. Colloids and Surfaces A: Physicochem Eng Aspects 2012; 395:105-15.

[16] Shih CJ, Lin S, Sharma R, Strano MS, Blankschtein D. Understanding the pH-dependent behavior of graphene oxide aqueous solutions: a comparative experimental and molecular dynamics simulation study. Langmuir 2012; 28(1):235-41.

[17] Schneidman-Duhovny D, Inbar Y, Nussinov R, Wolfson HJ. PatchDock and SymmDock: servers for rigid and symmetric docking. Nucl Acids Res 2005; 33(suppl 2):W363-W367.

[18] Makarucha AJ, Todorova N, Yarovsky I. Nanomaterials in biological environment: a review of computer modelling studies. Eur Biophys J 2011; 40(2):103-15.

[19] Monticelli L, Salonen E, Ke PC, Vattulainen, I. Effects of carbon nanoparticles on lipid membranes: a molecular simulation perspective. Soft Matter 2009; 5:4433-45.

[20] Berendsen HJC, van der Spoel D, Drunen R. GROMACS: A message-passing parallel molecular dynamics implementation. Comput Phys Commun 1995; 91:43-56.

[21] Jorgensen WL, Tirado-Rives J. The OPLS [optimized potentials for liquid simulations] potential functions for proteins, energy minimizations for crystals of cyclic peptides and crambin. J Am Chem Soc 1988; 110(6):1657-66.

[22] Nosé S, Klein, ML. Constant pressure molecular dynamics for molecular systems. Mol Phys 1983; 50(5):1055-76.

[23] Parrinello M, Rahman NA. Polymorphic transitions in single crystals: A new molecular dynamics method. J Appl Phys 1981; 52(12):7182-91.

[24] Ewald P. Die Berechnung optischer und elektrostatischer Gitterpotentiale. Ann Phys 1921; 369:253-87.

[25] Humphrey W, Dalke A, Schulten K. VMD - Visual Molecular Dynamics. J Mol Graph 1996; 14:33-8.

[26] Axelsen PH, Harel M, Silman I, Sussman JL. Structure and dynamics of the active site gorge of acetylcholinesterase: synergistic use of molecular dynamics simulation and X-ray crystallography. Protein Sci 1994; 3(2):188-97.

[27] Xu Y, Colletier JP, Weik M, Jiang H, Moult J, Silman I, et al. Flexibility of aromatic residues in the active-site gorge of acetylcholinesterase: X-ray versus molecular dynamics. Biophys J 2008; 95:2500-11.

[28] Wang Z, Zhang K, Zhao J, Liu X Xing B. Adsorption and inhibition of butyrylcholinesterase by different engineered nanoparticles. Chemosphere 2010; 79(1):86-92.

[29] Raffaini G, Ganazzoli F. Surface topography effects in protein adsorption on nanostructured carbon allotropes. Langmuir 2013; in press.

[30] Dreyer DR, Park S, Bielawski CW, Ruoff RS. The chemistry of graphene oxide. Chem Soc Rev 2010; 39(1):228-40.

[31] Chakraborti S, Joshi P, Chakravarty D, Shanker V, Ansari ZA, Singh SP, et al. Interaction of polyethyleneimine-functionalized ZnO nanoparticles with bovine serum albumin. Langmuir 2012; 28(30):11142-52.

[32] Sanfins E, Dairou J, Hussain S, Busi F, Chaffotte AF, Rodrigues-Lima F, Dupret JM. Carbon black nanoparticles impair acetylation of aromatic amine carcinogens through inactivation of arylamine N-acetyltransferase enzymes. ACS Nano 2011; 5(6):4504-11.

[33] Albanese A, Chan WC. Effect of gold nanoparticle aggregation on cell uptake and toxicity. ACS Nano 2011; 5(7):5478-89.

[34] Asuri P, Karajanagi SS, Yang H, Yim T, Kane RS, Dordick JS. Increasing protein stability through control of the nanoscale environment. Langmuir 2006; 22(13):5833-6.

[35] Mu Q, Liu W, Xing Y, Zhou H, Li Z, Zhang Y, et al. Protein binding by functionalized multiwalled carbon nanotubes is governed by the surface chemistry of both parties and the nanotube diameter. J Phys Chem C 2008; 112(9):3300-7.

[36] Vertegel AA, Siegel RW, Dordick JS. Silica nanoparticle size influences the structure and enzymatic activity of adsorbed lysozyme. Langmuir 2004; 20(16):6800-7.

[37] Lundqvist M, Sethson I, Jonsson BH. Protein adsorption onto silica nanoparticles: conformational changes depend on the particles' curvature and the protein stability. Langmuir 2004; 20(24):10639-47.

[38] Diamantino TC, Almeida E, Soares AM, Guilhermino L. Characterization of cholinesterases from *Daphnia magna* straus and their inhibition by zinc. Bull Environ Contam Toxicol 2003; 71(2):219-25.

[39] Gnagey AL, Forte M, Rosenberry TL. Isolation and characterization of acetylcholinesterase from *Drosophila*. J Biol Chem 1987; 262(27):13290-8.

[40] Thompson HM. Esterases as markers of exposure to organophosphates and carbamates. Ecotoxicology 1999; 8(5):369-84.

[41] Varó I, Navarro JC, Amat F, Guilhermino L. Characterisation of cholinesterases and evaluation of the inhibitory potential of chlorpyrifos and dichlorvos to *Artemia salina* and *Artemia parthenogenetica*. Chemosphere 2002; 48(6):563-9.

[42] Greenblatt HM, Silman I, Sussman JL. Structural studies on vertebrate and invertebrate acetylcholinesterases and their complexes with functional ligands. Drug Dev Res 2000; 50(3-4):573-83.